Non-Rigid Registration meets Surface Reconstruction

Mohammad Rouhani
INRIA Rhône-Alpes
Grenoble
mohammad.rouhani@inria.fr

Edmond Boyer
INRIA Rhône-Alpes
Grenoble
edmond.boyer@inria.fr

Angel D. Sappa
Computer Vision Center
Barcelona
angel.sappa@cvc.uab.es

Abstract

Non rigid registration is an important task in computer vision with many applications in shape and motion modeling. A fundamental step of the registration is the data association between the source and the target sets. Such association proves difficult in practice, due to the discrete nature of the information and its corruption by various types of noise, e.g. outliers and missing data. In this paper we investigate the benefit of the implicit representations for the non-rigid registration of 3D point clouds. First, the target points are described with small quadratic patches that are blended through partition of unity weighting. Then, the discrete association between the source and the target can be replaced by a continuous distance field induced by the interface. By combining this distance field with a proper deformation term, the registration energy can be expressed in a linear least square form that is easy and fast to solve. This significantly eases the registration by avoiding direct association between points. Moreover, a hierarchical approach can be easily implemented by employing coarse-to-fine representations. Experimental results are provided for point clouds from multi-view data sets. The qualitative and quantitative comparisons show the outperformance and robustness of our framework.

1. Introduction

Point set registration is a fundamental issue in shape modeling with several applications in computer vision [16], robotics or computer graphics [32]. This is particularly true in the recent years, as the expansion of affordable 3D sensors and of efficient point based reconstruction techniques have made point cloud processing a popular research domain. Registering two point clouds consists in finding the best deformation that aligns the two sets. Existing works that tackle this problem can be classified with respect to the *deformation model* they consider to transform point sets and also to the *distance* they use to measure the similarity between point sets. From optimization point of view, the earlier defines a solution space while the latter builds an objective function to be minimized. Hence, both terms have strong influence on the convergence to a meaningful solution. In this paper we particularly focus on the distance term and investigate the benefit of implicit interfaces in the case of non-rigid registration.

Independently of the deformation model, that can exhibit various type of rigidity from (*rigid* to *non-rigid*), the distance measure between two point clouds fundamentally relies on the point association scheme that is devised over which point distances are evaluated. Most of the existing strategies in that respect are based on discrete point associations. Some use the Euclidean distance and associate closest points in a deterministic way, as in ICP [3], or in a probabilistic way, as in [15]. Others better approximate the real distances between the associated shapes by considering normal and curvature information as in [26]. All these distance estimations are very sensitive to noise and outliers and they are prone to errors with missing parts. Moreover, the minimization of these distance approximations often gets trapped in local minima.

In this work we experiment a flexible interface (Fig.1(b)) for non-rigid registration with the objective to alleviate the need for discrete point associations. This interface is an implicit function that can define a distance field around the target point set. Interface representations have been successfully used to rigidly register two point sets, e.g., [27] and we consider here the extension to the non-rigid case. The interface induces a gradient field hence relaxing the constraint for explicit point correspondences (see Fig.1(c)). In addition, the interface representation can be implemented in a coarse-to-fine manner in order to avoid local minima. Figure1$(c)-(d)$ illustrates this principle with first a coarse implicit interface that captures the global shape information and then gradually switches to a finer interface that accounts for more details of the shape. The main features of our approach are the following:

1. A new efficient formulation that solves non-rigid registration problem without requiring any correspondence.

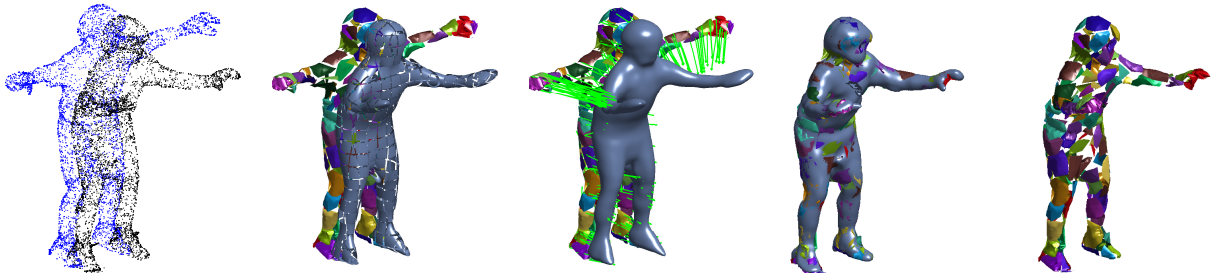

(a) *(b)* *(c)* *(d)* *(e)*

Figure 1. Using implicit interface for registration: (a) initial pose of the source and target sets; (b) source patches and the local quadrics representing the target; (c) the implicit interface induces a gradient field; (d) deformed source patches fitting the interface; a coarse-to-fine interface has been used in $(c) - (d)$; (e) the final deformation of the template.

2. The proposed representation allows for coarse to fine strategies in order to avoid local minima.

3. The resulting optimization can be performed by iteratively solving sparse linear system of equations.

4. The approach challenges traditional techniques that consider time consuming discrete point associations are prone to errors with noise, outliers and missing data

The remainder of the paper is as follows. Section 2 discusses related works in surface registration. The approach is detailed in Section 3 . Section 4 presents results and comparisons on public data sets.

2. Related Works

Point set registration consists in finding the best transformation that align two point sets in the same pose and in a single coordinate system. As mentioned earlier, the problem relies on two main aspects, namely the deformation model and the distance measurement. In this section the related works are presented with respect to these aspects.

Deformation model: such model should be defined prior to any rigid or non-rigid registration. Its importance comes from the fact that it defines the parameter space within which the optimization will be performed. It can be simply rigid or affine transformations that are linear with respect to the parameter vector allowing hence for only a few degrees of freedom. When it comes to non-rigid deformation, the model must be more elaborated in order to capture free form motions while the surface properties are preserved. These transformations can be divided in two main categories: the extrinsic and intrinsic deformations.

In the extrinsic deformation models, the whole space where the object is embedded undergoes a transformation and it deforms the object as well. For instance, in Thin-Plate Spline (TPS) [5], the space is deformed by changing the control weights of some radial basis functions. In Free-Form Deformation (FFD) [30] a mapping is provided by controlling the B-spline basis functions. Both transformations are widely used to model the deformation especially for medical imaging applications, where some region based information is available. The rigidity of these transformations is controlled by a quadratic regularization term that may penalize unnatural motions.

In contrast, the intrinsic deformation models, only consider the surface manifold. Changes are therefore applied directly on the points over the surface instead of the whole space. Laplacian deformation is one the most popular techniques in this category [31] that is widely used in motion capture applications, e.g. [1]. Local geometric properties (δ-coordinates) extracted at each vertex are assumed to be preserved during the transformation. Skinning methods like [18] use embedded skeleton and preserve the distances to the bone during the deformation, while [13] and [28] try to preserve isometric distances between the points.

In our approach, following [6] and [7], the non-rigid deformation is modeled as a combination of locally rigid transformations, which are applied to the small patches on the manifold. However, in order to reach a meaningful result, the compatibility of these local rigid patches must be maintained using some regularization term. For instance, [2] uses a naive stiffness term that imposes the similarity between the neighboring affine matrices. Instead, we consider a very simple rigidity term, proposed in [7], that checks the transformation effects of each patch on its neighbors. This choice hands over a quadratic deformation term that forces the patches to move together, as it is explained in Section 3.

Li et al. in [20] employ a similar approach in order to capture non-rigid deformation through the local rigid transformations. Firstly, a deformation graph is considered by a uniformly sampling over the source mesh. Then, each point undergoes an affine transformation that affects the neighboring points; this influence is measured in a similar way as [2]. After applying these local deformations, the whole mesh is undergoes a global rigid transformation. This model has been improved in [19] after replacing the uniform sampling by a temporally adaptive distribution that refines

the deformation graph. Articulated models are described in [9] through a set of rigid transformations that are associated to each point using skinning weights.

Data association: this is another major aspect to be considered as it defines the distance between the source and target. Many surface matching approaches employ features like spin images [16] or heat kernel signatures [32] for solving the assignment problem. However, in this work we only consider the spatial coordinates of the points. Iterative Closest Point (ICP) [3] is the most popular technique in that respect, where every source point is paired with its closest corresponding point in the target set for minimizing the accumulated distance. This distance might not be very accurate due to missing points for instance. In [10] and [25] further geometric information including normals and curvatures are exploited for better distance estimations. The authors in [19] employed a combination of point-to-point and point-to-plane distances for developing a fitting energy term in non-rigid registration.

Distance fields are also frequently used in order to accelerate the correspondence search. The distance transform and its derivatives are precomputed in a regular grid of voxels first [12]. The computation is still based on the discrete point associations and the accuracy depends on the grid size. Moreover, distance fields may fail in the presence of noise and missing parts. Probabilistic models, like Gaussian Mixture Model (GMM), are also popular for defining the distance [15]. In these models every point cloud is treated as a probabilistic distribution and the distance is defined as the correlation of two densities. This can be viewed as a sort of soft-assignment (e.g., RPM [11]) where many points in the target set are considered as the potential (weighted) correspondences of a single source point.

In our approach an implicit interface is used both for representing the target set and speeding up the distance computation. This work extends the rigid registration techniques in [27] and [35] to the non-rigid case by using a powerful implicit representation as the interface [24] in addition to a flexible deformation model. Unlike the aforementioned techniques, the proposed method does not require any correspondence search so that the computational cost is reduced. This approach is also robust to noise as it is handled twice, during the surface reconstruction and distance estimation. In addition, using the interface allows to perform coarse-to-fine estimations.

Optimization: Having designed a deformation model and a proper distance function, the optimization stage must be applied to minimize this term. This stage can be viewed as a search for the best parameters in the shape deformation space and its complexity depends on the designed energy term. In [12] a distance field has been used to estimate the distance during the rigid registration. The outcome is a function in the form of non-linear least squares that is solved through the Levenberg-Marquadt algorithm. Li et al. in [20, 19] apply this framework for minimizing a comprehensive energy term for non-rigid registration. In [29], the optimal TPS parameters are estimated by solving a nonlinear system of equations that are obtained through computing some proper integrals over the mesh. Gauss-Newton algorithm has been employed in [9] to find the rigid transformations of the articulated model; this is followed by another phase for assigning these rigid motions to the points.

Variational methods are also used to tackle the point set registration as an energy minimization problem. In [21] a finite-element method is used to solve a PDE of the warping field. Euler-Lagrange formulation has been employed in [35] to reach a smooth gradient field induced by an implicit polynomial. Gradient descent is one of the common techniques to find the optimal deformation in the nonlinear cases [17], [22]. Probabilistic approaches can be seen as an energy minimizing model as well; but, they use a different optimization framework. EM-like algorithm has been used in [23] to align two GMMs. Cagniart et al. in [8] have also employed this algorithm for improving the ICP algorithm presented in [7].

Linear least squares form, on the other hand, is one the simplest techniques in optimization that results in a closed form solution. In [26] a linear framework for registration is presented by using a curvature based distance estimation, but it still requires a discrete point association. In the current work, we aim at modeling the registration optimization in a least squares form that is easy and fast to solve. The proposed technique does not need any discrete point association due to the use of implicit interface. Both deformation and data terms are chosen in the way that can be easily optimized using a sparse system of linear equations. Furthermore, a hierarchical approach can be implemented by using coarse to fine interfaces to avoid local minima.

3. Non-Rigid Registration using Interface

In this section the proposed linear framework for the correspondence-free *non-rigid* registration is presented. First, an implicit interface is reconstructed to describe the target point cloud. Then, we explain how this interface can benefit the non-rigid registration by providing a new data term that avoids discrete point association. Finally, a sparse system of equation is derived in order to minimize our linear least squares function.

3.1. Implicit Interface

Implicit functions are among the most flexible representations for surface reconstruction that do not require any parameterization on the point cloud. These functions describe the objects of interest through their zero sets and provide further information around the objects. The description used in this work is based on small quadratic patches

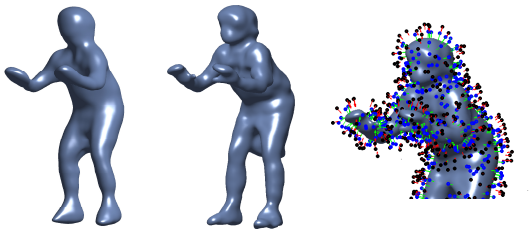

Figure 2. Using partition of unity for describing a point cloud: $(left)$ coarse; $(mid.)$ fine level; $(right)$ the induced gradient field.

that are reconstructed over the cells of an octree. The partition of unity technique is applied afterwards in order to provide a global implicit function that is smooth [24]. This interface provides high-level representations from coarse-to-fine, which can benefit the registration problem.

First of all, some small quadratic functions $\{f_1, f_2, ...\}$ are reconstructed to describe small patches of the target $\mathcal{T}$. Each function describes a small cell of an octree and can be further subdivided if more detail should be captured. Then, a smooth global function $\mathcal{F}$ can be reconstructed by blending these local patches:

$$\mathcal{F}(\mathbf{x}) = \sum_{i \in \mathcal{N}^{\mathbf{x}}} \hat{w}_i(\mathbf{x}) f_i(\mathbf{x}) \tag{1}$$

where $\mathcal{N}^{\mathbf{x}}$ refers to the set of octree cells in the neighborhood of $\mathbf{x}$. The weighting functions $\hat{w}_i(\mathbf{x})$ are calculated in each point using a radial function of the distance from the center of the cell. These weights must be normalized in order to sum up to one at any point. The global function $\mathcal{F}$ can be viewed as a convex combination of the quadratic patches that are blended in a smooth way. The influence of neighboring cells can be easily controlled through the blending radius defined in the weights [24]. Figure 1 illustrates how the patches are smoothly blended in different levels.

In this work, we are not interested in the visualization power of this reconstruction technique. We, instead, use this tool to obtain a continuous alternative to discrete point association. As illustrated in Fig.2$(right)$, this function induces a continuous gradient field whose vectors are pointing toward the object and their lengths are proportional to the distances. Taubin in [33], presents a good distance approximation that is used to define the data energy [27]:

$$E_{data}(\mathcal{S}, \mathbf{T}) = \sum_{\mathbf{x} \in \mathcal{S}} \left(\frac{\mathcal{F}(\mathbf{T}(\mathbf{x}))}{\|\nabla \mathcal{F}(\mathbf{T}(\mathbf{x}))\|} \right)^2 \tag{2}$$

where $\mathbf{T}$ is the optimal deformation to be applied on the source set. Instead of minimizing this non-linear term, a continuous form has been considered in [35] and the following gradient field is derived by applying calculus of variation:

$$\mathbf{g}(\mathbf{x}) = -\gamma \frac{\mathcal{F}(\mathbf{x})}{\|\nabla \mathcal{F}(\mathbf{x})\|^2} \nabla \mathcal{F}(\mathbf{x}). \tag{3}$$

Therefore, every point is associated with a vector along $\nabla \mathcal{F}$, which is orthogonal to the iso-surface, and its length is proportional to its distance from the zero set. This vector field has been exploited in the current work to develop a correspondence-free non-rigid registration framework.

3.2. Non-Rigid Registration

Correspondence-free registration based on the implicit interface has been already used in [27] and [35]. In these works only the *rigid* registration problem is considered, while we present a linear framework for tackling the *"non-rigid"* case using a highly flexible interface. Our formulation also allows a coarse-to-fine approach in order to avoid local minimums. This is accompanied with a flexible patch-based deformation model whose rigidity can be controlled by a quadratic term. As a consequence, a sparse system of linear equations can be derived to solve our correspondence-free non-rigid registration.

A non-rigid deformation can be simply modeled as a combination of local rigid transformations applied on the surface patches [2]. Indeed, the template surface is firstly clustered into small patches using a geodesic distance (Fig.1(b)). Let's $\mathbf{c}_i$ denote the center of the i-th patch. Then, non-rigid deformations can be easily modeled by applying local rigid transformations $\mathbf{T}_i(\mathbf{x}) = \mathbf{R}_i\mathbf{x} + \mathbf{t}_i$ over these patches. During the registration these rigid parameters can be updated through an affine perturbation that can be captured with 6 parameters denoted as $\boldsymbol{\omega}_i = (\mathbf{u}_i, \mathbf{v}_i)$:

$$\hat{\mathbf{T}}_i(\mathbf{x}) = \mathbf{T}_i(\mathbf{x}) + \mathbf{K}_i \boldsymbol{\omega}_i \tag{4}$$

where $\hat{\mathbf{T}}_i$ is the perturbed rigid transformation and $\mathbf{K}_i$ is the skew-symmetric matrix of $\boldsymbol{\beta} = \mathbf{R}_i(\mathbf{x} - \mathbf{c}_i)$ concatenated with the identity matrix [7]. In the rest of this section we show how to find the best affine parameters $\boldsymbol{\omega}_i$ and update the rigid transformations in order to minimize the data and deformation energy terms.

Data term: Thanks to the linear form of the update vector, the data term can be designed in the least squares form that benefits the optimization step. In the current work the gradient field in (3), induced by the implicit interface, is exploited to update the local rigid transformations. In fact, the source point in the current position $\mathbf{T}_i(\mathbf{x})$ must move along the gradient vector $\mathbf{g}(\mathbf{T}_i(\mathbf{x}))$ by minimizing the following term:

$$E_{data}(s) = \|\mathbf{K}_i \boldsymbol{\omega}_i - \mathbf{g}(\mathbf{T}_i(\mathbf{x}))\|^2. \tag{5}$$

This quadratic term is equivalent to imposing three linear constraints on every source point: $\mathbf{K}_i\boldsymbol{\omega}_i = \mathbf{g}(\mathbf{T}_i(\mathbf{x}))$. These constraints are only applied on those source points whose orientation in the current pose is quite similar to the gradient vector $\nabla \mathcal{F}$ at that point. This normal compatibility check avoids wrong correspondences. Moreover, through the distance estimation $d = |f|/\|\nabla f\|$ at every

source point, those points with the distance bigger than $2\sigma_d$ (standard deviation) are discarded as well.

Deformation term: The local rigid transformations result in a meaningful non-rigid deformation as long as the deformation energy can be controlled. Similar to [7] we penalize the incompatibility of any two neighboring rigid transformations as follows:

$$E_{deform}(\mathbf{T}) = \sum_{(\mathcal{P}^i,\mathcal{P}^j)\in\mathcal{N},\, \mathbf{x}\in\mathcal{P}^i\cup\mathcal{P}^j} E^{ij}(\mathbf{x}) \qquad (6)$$

where $\mathcal{N}$ is the set of all possible neighboring patches and each summand is defined for the points on the pair:

$$E^{ij}(\mathbf{x}) = \|\hat{\mathbf{T}}_i(\mathbf{x}) - \hat{\mathbf{T}}_j(\mathbf{x})\|^2. \qquad (7)$$

This term, in fact, measures the similarity of predictions between the rigid transformation of each patch and its neighboring patches. Following the notation in (4), this term can be described in the least squares form:

$$E^{ij}(\mathbf{x}) = \|\mathbf{K}_i\boldsymbol{\omega}_i - \mathbf{K}_j\boldsymbol{\omega}_j - (\mathbf{T}_j(\mathbf{x}) - \mathbf{T}_i(\mathbf{x}))\|^2. \qquad (8)$$

Sparse system: In each iteration we aim at finding the best $6N_{\mathcal{P}}$ affine parameters concatenated in the affine vector $\boldsymbol{\omega}$. The data and deformation terms are both in the quadratic form of $\boldsymbol{\omega}$; hence, minimizing the total energy $(E_{data} + \lambda E_{deform})$ is equivalent to solving an over-determined system of equations. The matrix A_1, corresponding to the data term, includes the entries of $\mathbf{K}_i$ and the right-hand value $\mathbf{b}_1$ contains the coordinates of the gradient field $\mathbf{g}(\mathbf{T}_i(\mathbf{x}))$. Similarly, another sparse matrix A_2 is constructed to express the deformation constraints applied for every point in a pair of patches; it includes the entries of $\mathbf{K}_i$ and $-\mathbf{K}_j$ according to (8). The right hand vector $\mathbf{b}_2$ includes the difference in predictions. Finally, the following system of linear equations must be solved to find the update vector:

$$\begin{bmatrix} A_1 \\ A_2 \end{bmatrix} \boldsymbol{\omega} = \begin{bmatrix} \mathbf{b}_1 \\ \mathbf{b}_2 \end{bmatrix}. \qquad (9)$$

After finding this vector, the closest rigid parameters must be found; so, the SVD decomposition is applied on the covariance matrix between the current points $\mathbf{T}(\mathcal{S})$ and updated position $\hat{\mathbf{T}}(\mathcal{S})$[1]. Then, every affine update $\mathbf{K}_i\boldsymbol{\omega}_i$ can be approximated by the proper rigid parameters $(\hat{\mathbf{R}}_i, \hat{\mathbf{t}}_\mathbf{i})$ to update the patch parameters:

$$\mathbf{R}_i := \hat{\mathbf{R}}_i\mathbf{R}_i, \qquad \mathbf{t}_\mathbf{i} := \hat{\mathbf{R}}_i\mathbf{t}_\mathbf{i} + \hat{\mathbf{t}}_\mathbf{i}. \qquad (10)$$

4. Experimental Results

The proposed registration framework has been validated for different data sets, which are either public [34] or obtained through a multi-view camera environment. The interfaces are reconstructed by the partition of unity weighting [24] applied on the quadratic patches acquired by [4]; octrees of depths $6, 7$ or 8 have been used for the representation. Figure 3(top) illustrates the implicit interfaces used for avoiding point association during the registration. It should be highlighted that these surfaces are reconstructed very fast (less than 1 second for 3K points).

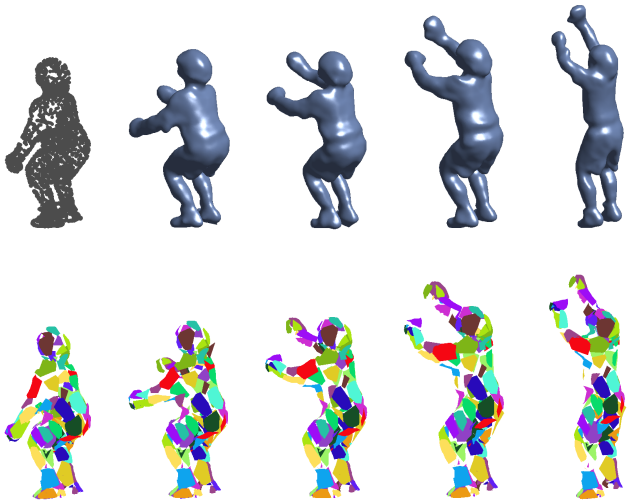

Figure 3. Using implicit interface for surface tracking: (top) the implicit interfaces; $(bottom)$ the deformed source patches; notice the patch colors to find out the correspondences.

Figure 3 and 4 illustrate the proposed framework for surface tracking for two sets of poses. Firstly, the template patches are constructed for the first frame by considering the geodesic distance on the surface. Then, implicit surfaces are reconstructed for other frames in order to lead the deformation. Each frame contains more than $30K$ points that are sub-sampled to $3K$. Note that this sub-sampling is only applied to save memory for the deformation term in (6); the employed surface reconstruction is able to describe the point clouds of high volume [24]. The last rows in Fig. 3-5 illustrate how the template patches deform rigidly following the gradient field induced by the interface.

Implicit surface reconstruction provides a high-level representation without requiring any parametrization. This fact has been exploited in this paper to benefit the registration problem. Figure 6 illustrates an example where the target set has some missing points that are properly interpolated after the reconstruction. In the case of noisy data set, one may use l^1-norm for quadric fitting before blending them through the partition of unity weighting [24]. The proposed framework is very flexible such that any implicit surface (partition of unity, B-splines [27]) can be used in any level from coarse to fine. This advantage can be exploited to implement a hierarchical approach in optimization. Figure 7 shows how the proposed framework leads to the global minimum while ICP-like methods may get stuck in some local minima.

[1] $\mathbf{T}(\mathcal{S}) = \{\mathbf{T}_i(\mathbf{x}), \mathbf{x}\in\mathcal{S}\}$; $\hat{\mathbf{T}}(\mathcal{S}) = \{\mathbf{T}_i(\mathbf{x}) + \mathbf{K}_i\boldsymbol{\omega}_i, \mathbf{x}\in\mathcal{S}\}$

Figure 4. 3D point registration using the proposed approach: (top) the implicit interfaces describing different frames $44, 49, 55, 75$; $(bottom)$ the deformed source patches.

The proposed approach has been quantitatively compared with four different registration methods as presented in Table 1. The accumulated registration error and the number of iterations for each case are presented in this table. The first and second columns correspond to [14] and [26], respectively, where FFDs have been used to model the transformation. In the earlier, the source and target sets are described by discrete distance transforms constructed in regular grids. This method is very slow since it requires some volume integral over the distance fields for computing the data term, which is minimized by gradient descent method.

ICP-like methods have been called for the comparisons in Table 1. In the second column a tangent based estimation is used for distance measurement in order to find the FFD parameters [26], while in the third column ICP is used to find the local rigid parameters [7]. ICP-like methods depend on a naive point association so they are very likely to get trapped in local minima (see Fig. 7). Finally, a probabilistic error based on the Gaussian Mixture Model (GMM) [15] has been used as the last quantitative comparison. This method uses TPS warping for modeling the deformation and it avoids explicit point association by applying an EM algorithm. This method is quite slow since all the source point are used as TPS control points and EM algorithm is repeated inside every iteration.

Table 1 shows how our method outperforms in terms of error and number of iterations. The accumulated errors in the last three rows are easily calculated since the ground truth correspondences are provided by [34]. For the first two rows, we use the distance from every target point to the tangent plane of its closest source point; it can be better estimated by using curvature information though [25]. The main advantage of our method is to work in a higher level representation than the point level. This enables us to have a general description of the point cloud in the coarser levels and add more details using the finer levels.

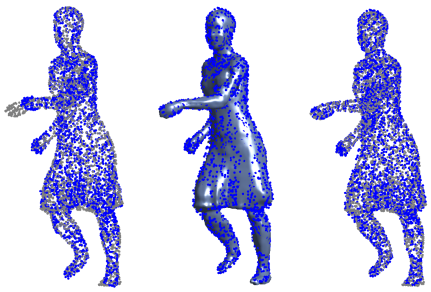

Figure 7. ICP approach in $(left)$ easily gets stuck in a local minima, while using interfaces leads to the global minimum $(right)$.

A qualitative comparison between different methods is presented in Fig. 8 for a quite challenging case, where the source pose is almost orthogonal to the target. Therefore, it is very likely that local methods get stuck in some local minima. The first two methods correspond to the linear assignment and coherent point drift [23]. The last three, all use the locally-rigid deformation model though they end with different results. Among all, EM algorithm [7] has shown a similar result to our approach after 500 iterations while ours has converged in only 30 iterations. In order to handle our correspondence-free algorithm we initialize a very coarse interface and switched to a finer one after 15 iterations.

5. Conclusions

In this paper a novel approach for non-rigid registration between two clouds of points has been proposed. The main contribution of this work is to consider the problem in higher level representations, where the source set is clustered into small patches that can deform rigidly, and the target is reconstructed by an implicit interface. Hence, the original problem in the point level is converted into a patches-to-interface problem without requiring any explicit point correspondence. Moreover, the use of implicit interface allows a coarse-to-fine approach that avoids local minimums. The presented method converges in few iterations, in which a sparse system of equations must be solved. The experimental results also illustrate the outperformance in the convergence and the robustness to the noise, outliers and missing parts in the target set.

Acknowledgment

This work was funded by the Seventh Framework Programme EU project RE@CT (grant agreement no. 288369). It was also supported in part by the TIN2011-25606 project.

References

[1] E. Aguiar, C. Stoll, C. Theobalt, N. Ahmed, H.-P. Seidel, and S. Thrun. Performance capture from sparse multi-view

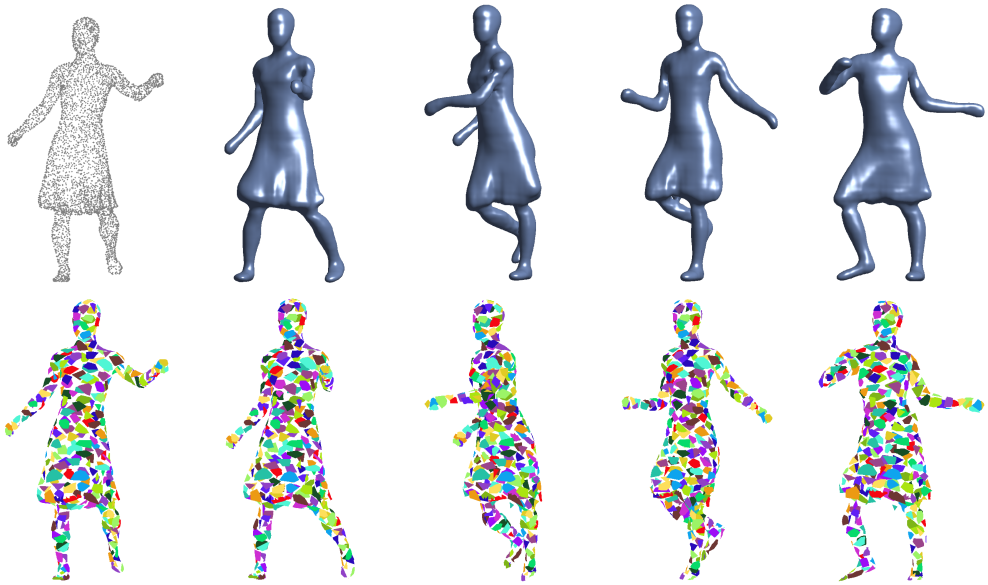

Figure 5. 3D point registration using the proposed approach: (top) the implicit interfaces describing different frames $46, 50, 56, 76, 91$; $(bottom)$ the deformed source patches.

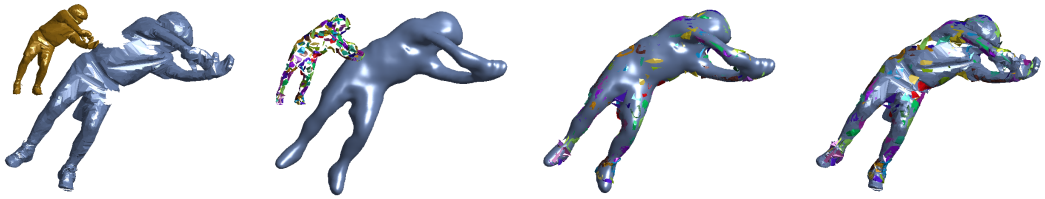

Figure 6. Tackle missing data: (a) the initial pose; (b) the implicit interface interpolates the target point cloud; (c) the source patches are moved toward the interface; (d) the converged pose of source patches.

video. *ACM TOG*, 27(3), 2008. 2

[2] B. Amberg, S. Romdhani, and T. Vetter. Optimal step nonrigid ICP algorithms for surface registration. *CVPR*, June 2007. 2, 4

[3] P. Besl and N. McKay. A method for registration of 3-d shapes. *IEEE PAMI*, 14(2):239–256, 1992. 1, 3

[4] M. Blane, Z. Lei, H. Çivi, and D. Cooper. The 3l algorithm for fitting implicit polynomial curves and surfaces to data. *IEEE PAMI*, 22(3):298–313, 2000. 5

[5] F. Bookstein. Principal warps: Thin-plate splines and the decomposition of deformations. *IEEE PAMI*, 11(6):567–585, 1989. 2

[6] M. Botsch, M. Pauly, M. Wicke, and M. Gross. Adaptive space deformations based on rigid cells. *Computer Graphics forum*, 26(3):339–347, 2007. 2

[7] C. Cagniart, E. Boyer, and S. Ilic. Free-form mesh tracking: A patch-based approach. *CVPR*, pages 1339–1346, 2010. 2, 3, 4, 5, 6, 8

[8] C. Cagniart, E. Boyer, and S. Ilic. Probabilistic deformable surface tracking from multiple videos. In *ECCV*, pages 326–339, 2010. 3, 8

[9] W. Chang and M. Zwicker. Global registration of dynamic range scans for articulated model reconstruction. *ACM TOG*, 30(3):26, 2011. 3

[10] Y. Chen and G. Medioni. Object modelling by registration of multiple range images. *Image Vision Computing*, 10(3):145–155, 1992. 3

[11] H. Chui and A. Rangarajan. A new point matching algorithm for non-rigid registration. *CVIU*, 89(2-3):114–141, 2003. 3

[12] A. Fitzgibbon. Robust registration of 2d and 3d point sets. *Image Vision Computing*, 21(13-14):1145–1153, 2001. 3

[13] Q.-X. Huang, B. Adams, M. Wicke, and L. Guibas. Non-rigid registration under isometric deformations. *Computer Graphics forum*, 27(5):1449–1457, 2008. 2

[14] X. Huang, N. Paragios, and D. Metaxas. Shape registration in implicit spaces using information theory and free form deformations. *IEEE PAMI*, 28(8):1303–1318, 2006. 6, 8

[15] B. Jian and B. Vemuri. Robust point set registration using Gaussian mixture models. *IEEE PAMI*, 33(8):1633–1645, 2011. 1, 3, 6, 8

[16] A. Johnson and M. Hebert. Using spin images for efficient object recognition in cluttered 3d scenes. *IEEE PAMI*, 21(5):433–449, 1999. 3

[17] T.-Y. Lee and S.-H. Lai. 3d non-rigid registration for mpu implicit surfaces. *CVPR Workshop*, pages 1–8, 2008. 3

(a) *(b)* *(c)* *(d)* *(e)* *(f)*

Figure 8. Qualitative comparison: (a): initial pose; (b): Linear assignment; (c): Coherent Point Drift [23]; (d): ICP with locally rigid deformation [7]; (e): EM with locally rigid deformation [8]; (f): Our result.

Table 1. Comparisons of non-rigid shape registration algorithms: **DT-FFD**: Distance Transform with FFD deformation [14]; **TD-FFD**: Tangent Distance approximation with FFD [26]; **ICP-LR**: Iterative Closest Point with Locally Rigid deformation [7]; **GMM-TPS**: Gaussian Mixture Model with TPS deformation [15] and the proposed approach.

	DT-FFD		TD-FFD		ICP-LR		GMM-TPS		Prop. App.:	
Figure	*Error*	*#Itr*	*Error*	*#Itr*	*Error*	*#Itr*	*Error*	*#Itr*	*Error*	*#Itr*
Fig.4	46.01	*16*	72.26	*30*	49.16	*28*	99.29	*20*	26.40	*24*
Fig.6	46.22	*18*	47.42	*18*	39.76	*18*	57.52	*25*	28.50	*18*
Fig.5$(1-2)$	20.83	*15*	21.99	*27*	9.70	*21*	12.10	*26*	7.34	*14*
Fig.5$(2-3)$	35.76	*22*	38.37	*30*	17.34	*25*	25.10	*39*	13.74	*21*
Fig.8	85.23	*30*	92.89	*30*	130.28	*30*	57.70	*31*	27.71	*30*

[18] J. Lewis, M. Cordner, and N. Fong. Pose space deformation: a unified approach to shape interpolation and skeleton-driven deformation. In *SIGGRAPH*, pages 165–172, 2000. 2

[19] H. Li, B. Adams, L. Guibas, and M. Pauly. Robust single-view geometry and motion reconstruction. *ACM TOG*, 28(5), 2009. 2, 3

[20] H. Li, R. Sumner, and M. Pauly. Global correspondence optimization for non-rigid registration of depth scans. *Computer Graphics forum*, 27(5):1421–1430, 2008. 2, 3

[21] S. Makram-Ebeid and O. Somphone. Non-rigid image registration using a hierarchical partition of unity finite element method. *ICCV*, pages 1–8, 2007. 3

[22] H. Munim, A. Farag, and A. Farag. Shape representation and registration in vector implicit spaces: Adopting a closed-form solution in the optimization process. *IEEE PAMI*, 35(3):763–768, 2013. 3

[23] A. Myronenko and X. Song. Point set registration: Coherent point drift. *IEEE PAMI*, 32(12):2262–2275, 2010. 3, 6, 8

[24] Y. Ohtake, A. Belyaev, M. Alexa, G. Turk, and H.-P. Seidel. Multi-level partition of unity implicits. *ACM TOG*, 22(3):463–470, 2003. 3, 4, 5

[25] H. Pottmann, S. Leopoldseder, and M. Hofer. Registration without ICP. *CVIU*, 95(1):54–71, 2004. 3, 6

[26] M. Rouhani and A. Sappa. Non-rigid shape registration: A single linear least squares framework. *ECCV*, pages 264–277, 2012. 1, 3, 6, 8

[27] M. Rouhani and A. Sappa. The richer representation the better registration. *IEEE TIP*, pages 5036–5049, 2013. 1, 3, 4, 5

[28] M. Salzmann, J. Pilet, S. Ilic, and P. Fua. Surface deformation models for nonrigid 3d shape recovery. *IEEE PAMI*, 29(8):1481–1487, 2007. 2

[29] Z. Santa and Z. Kato. Correspondence-less non-rigid registration of triangular surface meshes. *CVPR*, pages 2275–2282, 2013. 3

[30] T. Sederberg and S. Parry. Free-form deformation of solid geometric models. *SIGGRAPH*, pages 151–160, August 1986. 2

[31] O. Sorkine, D. Cohen-Or, Y. Lipman, M. Alexa, C. Rössl, and H.-P. Seidel. Laplacian surface editing. *Symposium on Geometry Processing*, pages 175–184, 2004. 2

[32] J. Sun, M. Ovsjanikov, and L. Guibas. A concise and provably informative multi-scale signature based on heat diffusion. *Computer Graphics forum*, 28(5):1383–1392, 2009. 1, 3

[33] G. Taubin. Estimation of planar curves, surfaces, and nonplanar space curves defined by implicit equations with applications to edge and range image segmentation. *IEEE PAMI*, 13(11):1115–1138, 1991. 4

[34] D. Vlasic, I. Baran, W. Matusik, and J. Popovic. Articulated mesh animation from multi-view silhouettes. *ACM TOG*, 27(3), 2008. 5, 6

[35] B. Zheng, R. Ishikawa, J. Takamatsu, T. Oishi, and K. Ikeuchi. A coarse-to-fine IP-driven registration for pose estimation from single ultrasound image. *CVIU*, 117(12):1647–1658, 2013. 3, 4